Measurement of the Branching Ratio and Asymmetry of the Decay $\Xi^\circ \to \Sigma^\circ\gamma$

A. Alavi-Harati,[12] T. Alexopoulos,[12,*] M. Arenton,[11] K. Arisaka,[2] S. Averitte,[10] A. R. Barker,[5] L. Bellantoni,[7] A. Bellavance,[9] J. Belz,[10,†] R. Ben-David,[7] D. R. Bergman,[10] E. Blucher,[4] G. J. Bock,[7] C. Bown,[4] S. Bright,[4] E. Cheu,[1] S. Childress,[7] R. Coleman,[7] M. D. Corcoran,[9] G. Corti,[11] B. Cox,[11] M. B. Crisler,[7] A. R. Erwin,[12] R. Ford,[7] A. Glazov,[4] A. Golossanov,[11] G. Graham,[4] J. Graham,[4] K. Hagan,[11] E. Halkiadakis,[10] J. Hamm,[1] K. Hanagaki,[8,‡] S. Hidaka,[8] Y. B. Hsiung,[7] V. Jejer,[11] D. A. Jensen,[7] R. Kessler,[4] H. G. E. Kobrak,[3] J. LaDue,[5] A. Lath,[10] A. Ledovskoy,[11] P. L. McBride,[7] P. Mikelsons,[5] E. Monnier,[4,§] T. Nakaya,[7,‖] K. S. Nelson,[11] H. Nguyen,[7] V. O'Dell,[7] M. Pang,[7] R. Pordes,[7] V. Prasad,[4] B. Quinn,[4] , E. J. Ramberg,[7,¶] R. E. Ray,[7] A. Roodman,[4,**] M. Sadamoto,[8] S. Schnetzer,[10] K. Senyo,[8,††] P. Shanahan,[7] , P. S. Shawhan,[4,‡‡] J. Shields,[11] W. Slater,[2] N. Solomey,[4] S. V. Somalwar,[10] R. L. Stone,[10] I. Suzuki,[8,§§] E. C. Swallow,[4,6] S. A. Taegar,[1] , R. J. Tesarek,[10,§§] G. B. Thomson,[10] P. A. Toale,[5] A. Tripathi,[2] R. Tschirhart,[7] S. E. Turner,[2] Y. W. Wah,[4] J. Wang,[1] H. B. White,[7] J. Whitmore,[7] B. Winstein,[4] R. Winston,[4] T. Yamanaka,[8] and E. D. Zimmerman[4,‖‖]

(KTeV Collaboration)

[1]*University of Arizona, Tucson, Arizona 85721*
[2]*University of California at Los Angeles, Los Angeles, California 90095*
[3]*University of California at San Diego, La Jolla, California 92093*
[4]*The Enrico Fermi Institute, The University of Chicago, Chicago, Illinois 60637*
[5]*University of Colorado, Boulder, Colorado 80309*
[6]*Elmhurst College, Elmhurst, Illinois 60126*
[7]*Fermi National Accelerator Laboratory, Batavia, Illinois 60510*
[8]*Osaka University, Toyonaka, Osaka 560-0043 Japan*
[9]*Rice University, Houston, Texas 77005*
[10]*Rutgers University, Piscataway, New Jersey 08854*
[11]*The Department of Physics and Institute of Nuclear and Particle Physics, University of Virginia, Charlottesville, Virginia 22901*
[12]*University of Wisconsin, Madison, Wisconsin 53706*

(Received 11 December 2000)

We have studied the rare weak radiative hyperon decay $\Xi^\circ \to \Sigma^\circ\gamma$ in the KTeV experiment at Fermilab. We have identified 4045 signal events over a background of 804 events. The dominant $\Xi^\circ \to \Lambda\pi^\circ$ decay, which was used for normalization, is the only important background source. An analysis of the acceptance of both modes yields a branching ratio of $B(\Xi^\circ \to \Sigma^\circ\gamma)/B(\Xi^\circ \to \Lambda\pi^\circ) = (3.34 \pm 0.05 \pm 0.09) \times 10^{-3}$. By analyzing the final state decay distributions, we have also determined that the Σ° emission asymmetry parameter for this decay is $\alpha_{\Xi\Sigma} = -0.63 \pm 0.09$.

DOI: 10.1103/PhysRevLett.86.3239 PACS numbers: 13.30.Eg, 13.40.Hq, 14.20.Jn

We report here on the Fermilab KTeV experiment's analysis of the decay $\Xi^\circ \to \Sigma^\circ\gamma$. This is an example of one of the most intriguing classes of baryon decays—weak radiative hyperon decays (WRHD). These decays are experimentally quite accessible, having branching ratios on the order of 10^{-3} [1]. The two most significant variables that can be measured in these decays are the branching ratio (BR), and the asymmetry of the baryon emission with respect to the initial spin axis (α). However, despite this experimental simplicity, there is no known theoretical framework for explaining these decays. Some of the difficulty in explaining WRHD is because predictions using the quark model do not match predictions from an analysis at the hadron level [2].

Hara proved in 1964 that $\alpha = 0$ in the SU(3) limit for the Σ^+ and Ξ^- WRHD, assuming only CP invariance and U spin symmetry (s and d quark exchange symmetry) [3]. An estimate, based on single-quark $s \to d$ transitions and that takes into account SU(3) breaking predicts a modest positive asymmetry, with the magnitude depending on the assignment of quark masses [4]. However, the only asymmetry of any WRHD that has been measured accurately, the one for $\Sigma^+ \to p\gamma$, has been found to be highly negative, -0.76 ± 0.08 [5]. The corresponding branching ratio cannot be understood as being due to single-quark transition. A recent paper suggests that this large negative asymmetry could result from intermediate resonances in the decay, and gives a prediction of a positive asymmetry for the $\Xi^\circ \to \Sigma^\circ\gamma$ mode [6].

To constrain the theoretical models, it is vital to measure accurately the parameters of WRHD for hyperons other than the Σ^+. Reference [7] states that whether Hara's theorem can be incorporated into a successful theoretical model depends on the experimental results from the two Ξ° weak radiative decays.

The decay $\Xi^\circ \to \Sigma^\circ\gamma$ has been previously observed in two separate experiments [8,9]. Both experiments have sample sizes of less than 100 events. The most accurate

branching ratio is reported as $(3.6 \pm 0.4) \times 10^{-3}$ [8]. This experiment also reported an asymmetry measurement, but it is incorrect because the dependence of the Λ polarization on its decay angle was not taken into account.

Many of the details of the KTeV beam line, experiment, and hyperon trigger can be found in a previous publication [10]. We reemphasize here some of the details particularly relevant to this measurement. The beam line for KTeV was designed to deliver two square high intensity beams of K_L particles for CP violation studies. The detector is situated 94 m from the target. The sweeping magnets in the beam line were designed and operated so that the integrated magnetic field delivered Ξ° hyperons polarized (with about 10% polarization) in the positive or negative vertical direction. We reversed one of the magnets regularly so that the net polarization was zero for the data discussed here.

The detector consists of a 64 m long vacuum decay vessel followed by a spectrometer. The decay vessel contains several lead/scintillator vetos with square apertures in their center. These are used to veto events where decay particles leave the sensitive area of the detector. The vacuum vessel is followed by 4 drift chambers, two situated on either side of an analysis magnet. This magnetic spectrometer gives a momentum resolution for charged particles of $\sigma(P)/P = 0.38\% \oplus P \times 0.016\%$, where P is in GeV/c. Photon veto detectors surround each drift chamber station.

Downstream of the last drift chamber is a set of nine transition radiation detectors (TRD). A plane of vertically oriented trigger hodoscopes is situated after the last TRD chamber. This plane is followed by the electromagnetic calorimeter which is composed of an array of 3100 crystals of pure CsI, 27 radiation lengths deep. The energy resolution of the calorimeter for electrons and photons is approximately $\sigma(E)/E \approx 0.45\% \oplus 2\%/\sqrt{E}$ and the position resolution is approximately 1 mm.

There are two beam holes in the TRD radiators, the trigger counters and the calorimeter. After the calorimeter is a 10 cm thick lead wall and then a hodoscope array (HA), with a single beam hole encompassing both beams, which provides a veto for hadronic showers. This is followed by three steel walls and two hodoscope arrays, which provide a veto for muons. Two small scintillation counters are situated in the beam hole of the first steel wall to provide a trigger for highly forward going charged particles.

The final decay products of the $\Xi^\circ \to \Sigma^\circ\gamma$ signal are a proton in one of the beam holes and a π^- and two photons hitting the calorimeter. These are the same final decay products as for the normalization mode $\Xi^\circ \to \Lambda\pi^\circ$.

The trigger for the experiment is built on a standard multilevel architecture, with the level 1 incorporating fast triggering elements, level 2 being a somewhat slower and more detailed hardware trigger, and level 3 being a real time processing filter to select for specific decay modes. The main hyperon trigger was designed to measure the previously unobserved beta decay of the Ξ°. Further details can be found in the paper reporting its discovery [10]. Since this trigger vetoed on a signal of more than 2.5 MIP's in the HA array, it rejected 58% of the $\Xi^\circ \to \Sigma^\circ\gamma$ signal and $\Xi^\circ \to \Lambda\pi^\circ$ normalization mode because the final state π^- often showers in the CsI or lead. The momentum and position distributions of the π^- in the calorimeter are nearly identical for the signal and normalization mode. Because of this, there is little bias in the measurement of the branching ratio due to the hadronic veto. Below we discuss details of the systematic checks we have performed to verify this.

We established a set of offline selection cuts to accept both modes and another set of cuts to distinguish between the two. The cuts in common include the following. There are 2 charged tracks, with the higher momentum track positively charged and with momentum between 85 and 600 GeV/c. The lower momentum track is negative, with a momentum between 5 and 150 GeV/c and has an energy in the CsI calorimeter less than 90% of its momentum. The two tracks must have a momentum ratio greater than 3.5 and, assuming a proton and pion identity, must combine to form an invariant mass within 15 MeV/c^2 of the Λ mass. Each of the two calorimeter clusters is required to have at least 2 GeV of energy and no charged track pointing at it. The sum of the two energies must be at least 16 GeV. We also require that the two photons do not reconstruct as a π° within 3 m along the beam line direction of the charged track vertex.

We reconstruct the Λ flight path from the reconstructed momentum of the proton and pion tracks. To find the decay vertex of the parent Ξ°, we numerically vary the distance along the beam line, or z. For a Ξ° vertex at a given z, we calculate the transverse coordinates by extrapolating the Λ flight path back to that location. We choose the value of z that minimizes the difference between the reconstructed invariant mass of all the final state particles and the Ξ° mass. We discard events with a decay vertex outside of the vacuum decay region, which we define as $Z = 95$–155 m. Events are also discarded if the daughter Λ vertex falls upstream of the parent Ξ° vertex. We also require that the total reconstructed momentum (Λ plus two photons) transverse to the flight path of the Ξ° parent, or p_T^2, be less than 0.0005 GeV$^2/c^2$. In addition, we reconstruct the event as a decay of a Λ from the primary target and as a $\Xi^\circ \to \Lambda\gamma$ decay and discard the event if it is consistent with either.

The distinguishing characteristics between the signal and normalization decay modes reside in the invariant masses between pairs of the final state particles. For the signal mode, one of the $\Lambda\gamma$ combinations will reconstruct as a Σ°, while for the normalization mode the two gammas will reconstruct as a π°. Figure 1 shows these invariant mass combinations for the data. A cut of $|m_{\gamma\gamma} - m_{\pi^\circ}| < 20$ MeV/c^2 is made in this figure to make the signal mode visible. This cut reduces the signal mode by about 27%, but reduces the normalization mode

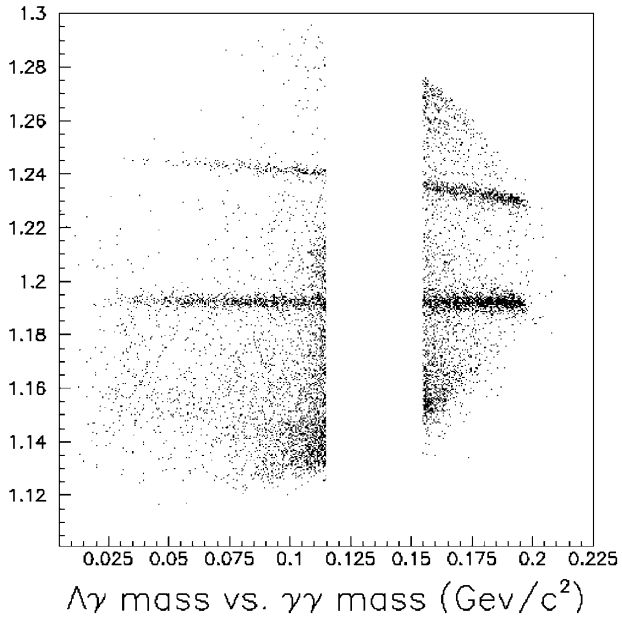

FIG. 1. A plot of Λ-γ mass versus γ-γ mass for all data.

by a factor of 180. A wider cut on the $\gamma\gamma$ mass does not significantly improve the signal to background ratio. The lower energy photon is chosen to be paired with the Λ in the figure. The presence of a Σ° mass band can be seen in this plot along with the band arising from the incorrect pairing of the photon.

Figure 2 shows the final invariant $\Lambda\gamma$ mass plot (a projection of Fig. 1), with the photon chosen to give the lowest mass. The background under the Σ° mass peak can

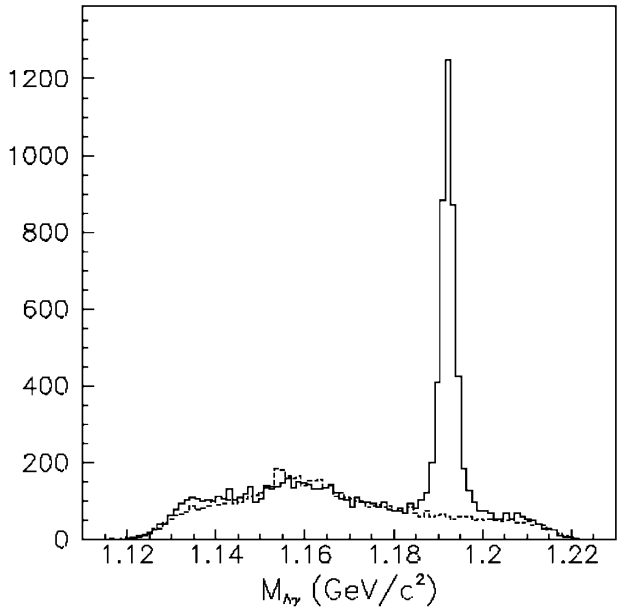

FIG. 2. A plot of the Λ-γ invariant mass for all data events passing selection cuts. Superimposed is normal mode Monte Carlo events that pass the selection cuts. This latter distribution is scaled to fit the data.

be explained entirely by the normalization mode decays $\Xi^\circ \to \Lambda\pi^\circ$ that fall outside of our $\gamma\gamma$ mass cut. We fit the distribution in Fig. 2 above a mass value of 1.16 GeV/c^2 to a Monte Carlo simulation of the $\Xi^\circ \to \Sigma^\circ\gamma$ signal and $\Xi^\circ \to \Lambda\pi^\circ$ background. The relative level of the background has been allowed to float in the fit since the simulation is not guaranteed to be accurate in describing the population at the extreme tails of the π° mass peak. The fit level is about 25% higher than indicated by the number of well reconstructed normalization mode decays.

As can be seen in Fig. 2, the simulated background describes the data very well. We subtract the simulated background distribution from the data and count the number of events in the Σ° mass region of 1185–1201 MeV/c^2. For our data, this is 4045 events, which gives a statistical uncertainty of ± 64 events. The number of background events in this region as estimated by the background fit is 804 events, giving a signal to background ratio of 5:1. The number of normalization events in our data is 1 377 642. There is a negligible amount of background for the normalization mode. Using the simulation of the detector, we determine that the ratio of acceptances for the signal decay mode to the normalization decay mode is 0.88. The acceptance does not depend significantly on the asymmetry parameter used. This results in a branching ratio measurement of $B(\Xi^\circ \to \Sigma^\circ\gamma)/B(\Xi^\circ \to \Lambda\pi^\circ) = (3.34 \pm 0.05) \times 10^{-3}$ where the error quoted is purely statistical.

The two largest systematic effects on the calculation of the branching ratio are background and acceptance uncertainties. The statistical error on the amount of background is 28. We varied the region around the signal mass peak in which to fit the simulated background and obtained an uncertainty of 40 events in the signal region due to the level of the fit. Additionally, looking at comparisons between event variables for those background events in the Σ° mass peak sidebands, we can see small discrepancies between the simulation and the data. We conservatively estimate that at most 60 background events could be unaccounted for under the signal peak. In all, we assign an uncertainty of 80 events to the amount of background, giving an uncertainty in the branching ratio of $\pm 0.07 \times 10^{-3}$.

The uncertainty in the acceptances is primarily due to the fact that we do not simulate hadronic showering in the HA detector and thus do not account for this effect at the trigger level. The effect of the hadronic veto on the absolute level of our signal is substantial. However, because the normalization mode has the identical final state, this effect cancels out in the branching ratio calculation. We find that the kinematic distributions relevant to the HA detector (such as pion and proton position and momentum) are very similar between the signal and normalization decay modes. We tested a simple model of hadronic vetoing in the Monte Carlo containing both position and momentum dependence for the π^-. We observed that the ratio of acceptances between signal and normalization did not

change at all. We assign a value of $\pm 0.05 \times 10^{-3}$ branching ratio uncertainty due to the hadronic veto. We explored the sensitivity to analysis cuts by varying the three most relevant variables: p_T^2, the z range for the Ξ°, and the separation of the Ξ° and Λ vertices. The variation seen from these cuts matches the level of uncertainty from the other sources quoted above. We also broke the data into various subsets (left vs right beam, and run number) and find the individual results statistically consistent.

The final systematic uncertainty in the branching ratio from the above sources is $\pm 0.09 \times 10^{-3}$. This then gives the final branching ratio result of $B(\Xi^\circ \to \Sigma^\circ\gamma)/B(\Xi^\circ \to \Lambda\pi^\circ) = (3.34 \pm 0.05 \pm 0.09) \times 10^{-3}$.

A value of the asymmetry parameter, $\alpha_{\Xi\Sigma}$, has also been obtained from our data. This parameter is determined most directly from the up-down asymmetry in the decay distribution of polarized Ξ°'s. However, our low degree of polarization ($\approx$10%) limits the power of this approach. For an unpolarized initial Ξ° state, as in our total data sample, angular momentum considerations dictate that the longitudinal polarization of the decay Σ° is just $-\alpha_{\Xi\Sigma}$ [11]. In the subsequent electromagnetic decay, the Λ retains the component of the parent Σ° polarization along the Λ direction of motion, but with opposite sign. The final $\Lambda \to p\pi^-$ weak decay asymmetry ($\alpha_{\Lambda p} = 0.642$ [1]) then analyzes the polarization. The resulting proton angular distribution is thus proportional to $[1 + \alpha_{\Xi\Sigma}\alpha_{\Lambda p}\cos(\theta_{\Sigma\Lambda})\cos(\theta_{\Lambda p})]$, where the angles are determined in the rest frame of each decaying particle. All of these angles can be determined in our data.

If one ignores the decay $\Sigma^\circ \to \Lambda\gamma$ and simply averages over all directions of the Λ emission, then the net asymmetry seen will be diluted by a factor of $-1/3$, assuming that experimental acceptance does not affect the decay asymmetrically. It should be noted that the previous measurement of asymmetry in the decay $\Xi^\circ \to \Sigma^\circ\gamma$ did not take into account this dilution [8].

In our analysis, we consider the two-dimensional distribution of the cosines described above. We measure the rest frame angles for each event and then perform a χ^2 comparison between the distribution seen in data with that for Monte Carlo, using different values of the asymmetry parameter in the generation. We used a 5 bin $\times$ 5 bin construction. A row of 5 bins is virtually empty due to the cut made on the π° mass so we do not use these bins in the χ^2 calculation. We made 11 separate Monte Carlo samples using different values of the asymmetry parameter, ranging from $\alpha_{\Xi\Sigma} = 0.0$ to $\alpha_{\Xi\Sigma} = -1.0$. An estimate for the background was determined bin-by-bin from the Monte Carlo. The χ^2 between the background subtracted data and the Monte Carlo signal distribution was calculated for each of these cases and the result is shown in Fig. 3. A fit to this curve with a parabola gives a minimum at $\alpha_{\Xi\Sigma} = -0.63$, with a corresponding value of χ^2 of 27.7 for 18 degrees of freedom. The 1 unit variation of χ^2 gives an error on this measurement of ± 0.08.

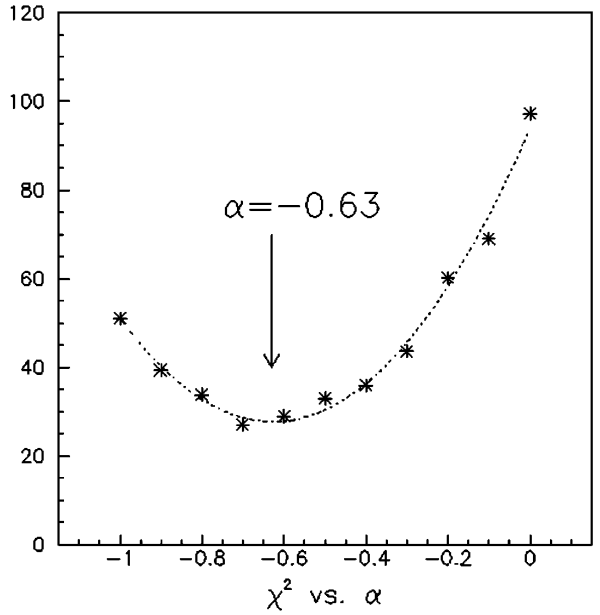

FIG. 3. The plot of χ^2/d.o.f. comparison of background subtracted data cosine distributions to the Monte Carlo. The 2nd degree polynomial fit is shown, with the minimum at $\alpha = -0.63$ identified.

Several tests were done to see if there are systematic effects on this result for the asymmetry parameter. To test the effect of background on the result for asymmetry, we repeated the analysis described above without background subtraction. The result is $\alpha_{\Xi\Sigma} = -0.66 \pm 0.08$, which does not vary significantly from the background subtracted value. The main difference is that the χ^2/d.o.f. at the minimum increases from 1.5 to 2.8. To test whether the beam hole region had an effect on the calculation of the asymmetry value, we applied the additional requirement that the pion does not hit the region of the calorimeter between the beam holes. We then repeated the χ^2 analysis. The result is $\alpha_{\Xi\Sigma} = -0.67 \pm 0.08$ with the χ^2/d.o.f. at the minimum of 1.5. We also calculated the χ^2 fit for comparisons with the Monte Carlo data without HA simulation and found no significant difference. We estimate that the systematic error on the asymmetry measurement is ± 0.05, yielding our final result, $\alpha_{\Xi\Sigma} = -0.63 \pm 0.08 \pm 0.05$. We independently verified the sign and magnitude of this asymmetry by directly comparing our two oppositely polarized samples of data.

This result is only the second measurement making an accurate determination of a WRHD asymmetry. The value of the decay asymmetry is highly negative, similar to that seen in the decay $\Sigma^+ \to p\gamma$.

We gratefully acknowledge the support and effort of the Fermilab staff and the technical staffs of the participating institutions for their vital contributions. This work was supported in part by the U.S. Department of Energy, The National Science Foundation, and The Ministry of Education and Science of Japan. In addition, A. R. B., E. B., and S. V. S. acknowledge support from the NYI program of the

NSF; A. R. B. and E. B. from the Alfred P. Sloan Foundation; E. B. from the OJI program of the DOE; K. H., T. N., and M. S. from the Japan Society for the Promotion of Science.

*Present address: National Technical University, 175 73 Athens, Greece.
†Present address: Montana State University, Bozeman, Montana 59717.
‡Present address: Princeton University, Princeton, New Jersey 08544.
§On leave from C.P.P. Marseille/C.N.R.S., France.
‖Present address: Kyoto University, 606-8502 Japan.
¶To whom all correspondence should be addressed.
**Present address: Stanford Linear Accelerator Center, Stanford, California 94309.
††Present address: Nagoya University, Nagoya 464-8602 Japan.
‡‡Present address: California Institute of Technology, Pasadena, California 91125.
§§Present address: Fermi National Accelerator Laboratory, Batavia, Illinois 60510.
‖‖Present address: Columbia University, New York, New York 10027.

[1] Particle Data Group, Z. Phys. C **3** (2000). Note that to avoid confusion we use the symbol $\alpha_{\Xi\Sigma}$ for the decay baryon asymmetry parameter. This is generically defined as α_γ on p. 694 of this reference.
[2] For a general review of the experimental and theoretical issues of WRHD, see J. Lach and P. Zenczykowski, Int. J. Mod. Phys. A **10**, 3817 (1995).
[3] Y. Hara, Phys. Rev. Lett. **12**, 378 (1964).
[4] N. Vasanti, Phys. Rev. D **13**, 1889 (1976).
[5] M. Foucher *et al.,* Phys. Rev. Lett. **68**, 3004 (1992).
[6] B. Borasoy and B. Holstein, Phys. Rev. D **59**, 054019 (1999). See also M. B. Gavela *et al.,* Phys. Lett. B **101**, 417 (1981), where the prediction for the $\Xi^\circ \to \Sigma^\circ\gamma$ asymmetry using a similar model is negative.
[7] P. Zenczykowski, Phys. Rev. D **62**, 014030 (2000).
[8] S. Teige *et al.,* Phys. Rev. Lett. **63**, 2717 (1989).
[9] V. Fanti *et al.,* Eur. Phys. J. C **12**, 69 (2000).
[10] A. Affolder *et al.,* Phys. Rev. Lett. **82**, 3751 (1999).
[11] See R. E. Behrends, Phys. Rev. **111**, 1691 (1958), for a discussion of asymmetries in radiative hyperon decays.